



Cite this: *Dalton Trans.*, 2020, **49**, 16238

Rapid mechanochemical synthesis of metal–organic frameworks using exogenous organic base†

Zihao Wang, Zongzhe Li, Marcus Ng and Phillip J. Milner *
Published on 29 April 2020. Downloaded on 05/01/2026 23:52:27.

Metal–organic frameworks (MOFs) bearing coordinatively unsaturated metal centers, exemplified by the MOF-74 family of frameworks, are promising for applications ranging from gas separations and storage to Lewis acid catalysis. However, the scalable synthesis of MOF-74 analogues remains a significant challenge. Recently, mechanochemistry has emerged as a sustainable strategy for the preparation of MOFs in the solid state with minimal solvent waste. Mechanochemical methods typically rely on metal salts bearing basic anions to deprotonate the conjugate acid of the organic linker and a small amount of organic solvent or water to facilitate liquid assisted grinding. Here, we demonstrate that the liquid exogenous organic base Hünig's base (*N,N*-diisopropylethylamine) can fulfill both roles, enabling the mechanochemical synthesis of $M_2(\text{dobdc})$ analogues ($M = \text{Mg, Mn, Co, Ni, Cu, Zn}$; $\text{dobdc}^{4-} = 2,5\text{-dioxidobenzene-1,4-dicarboxylate}$) using metal nitrate salts in only 5 minutes at room temperature. Importantly, we demonstrate that this straightforward method can be generalized to prepare the isomeric framework $\text{Mg}_2(m\text{-dobdc})$ ($m\text{-dobdc}^{4-} = 2,4\text{-dioxidobenzene-1,5-dicarboxylate}$) and the expanded framework $\text{Mg}_2(\text{dobpdc})$ ($\text{dobpdc}^{4-} = 4,4'\text{-dioxidobiphenyl-3,3'-dicarboxylate}$) under solvent-free conditions for the first time. The MOFs prepared using this method possess high crystallinities and surface areas, with the $\text{Mg}_2(m\text{-dobdc})$ prepared herein representing the first reported permanently porous variant of this framework. This new sustainable mechanochemical synthesis of MOF-74 analogues should enable their preparation on a large scale for industrial applications.

Received 3rd April 2020,
Accepted 29th April 2020
DOI: 10.1039/d0dt01240h
rsc.li/dalton

Introduction

Metal–organic frameworks (MOFs) are a class of porous, crystalline solids constructed from polytopic organic “linkers” and inorganic “secondary building units” (SBUs) with myriad potential applications ranging from chemical separations to catalysis.^{1,2} Of these, MOFs bearing coordinatively unsaturated or open metal centers are particularly intriguing due to their ability to strongly polarize and bind guest molecules.³ In addition, MOFs with open metal centers are promising heterogeneous Lewis acid catalysts.^{4,5} Among open metal site MOFs, the MOF-74 or CPO-27 family stands out in terms of structural tunability and density of open metal sites (Fig. 1).⁶ Following the initial report of the synthesis of $\text{Zn}_2(\text{dobdc})$ ($\text{dobdc}^{4-} = 2,5\text{-dioxidobenzene-1,4-dicarboxylate}$) in 2005,⁶ several isostructural metal analogues, including Mg ,⁷ Mn ,⁸ Co ,⁹ Ni ,¹⁰ and Cu ,^{11,12} congeners, as well as isomeric¹³ and expanded^{14–21} var-

iants, have been reported (Fig. 1). Due to their hexagonal one-dimensional channels lined with a high density of five-coordinate M^{2+} centers, activated MOF-74 variants hold numerous records for gas storage capacities at low pressures, including for CO_2 and H_2 .^{12,22} In addition, MOF-74 analogues demonstrate promising catalytic activity for Lewis acid-mediated^{23,24} and C–H oxidation reactions.^{17,25} Given the promise of MOF-74 analogues for industrial applications, sustainable methods for their preparation on scale are desirable.^{26,27}

As with many MOFs, MOF-74 analogues are typically prepared under ultra-dilute solvothermal conditions using amide solvents such as *N,N*-dimethylformamide (DMF) (Fig. 2a).^{28,29} The role of the amide solvent is to decompose at high temperatures ($>100\text{ }^\circ\text{C}$) to produce amines (e.g. *N,N*-dimethylamine) that deprotonate the conjugate acid of the linker prior to MOF self-assembly. While these solvothermal syntheses produce highly crystalline frameworks,¹² they employ solvents that are undesirable on industrial scale²⁹ and result in significant generation of organic waste. In addition, a lack of control over the strength of the base and the rate of its addition limits the inherent synthetic tunability of these methods. This is important because parameters such as pH and temperature can have

Department of Chemistry and Chemical Biology, Cornell University, Ithaca, NY 14853, USA. E-mail: pjm347@cornell.edu

† Electronic supplementary information (ESI) available. See DOI: [10.1039/d0dt01240h](https://doi.org/10.1039/d0dt01240h)

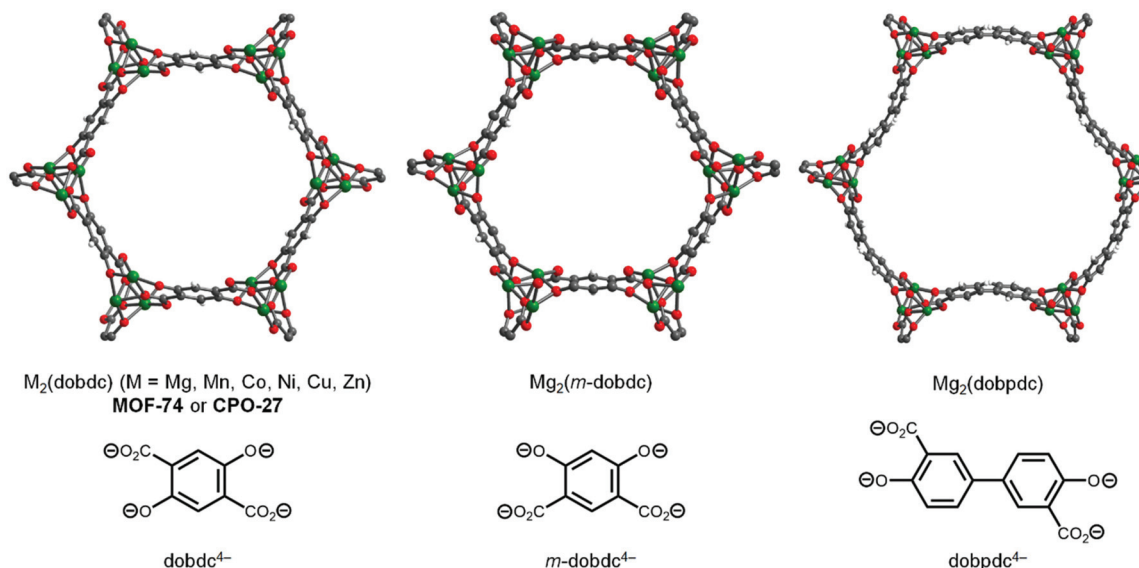


Fig. 1 Structures of the open metal site metal–organic frameworks $M_2(\text{dobdc})$ ($M = \text{Mg, Mn, Co, Ni, Cu, Zn}$; $\text{dobdc}^{4-} = 2,5\text{-dioxido-1,4-dicarboxylate}$), $\text{Mg}_2(m\text{-dobdc})$ ($m\text{-dobdc}^{4-} = 2,4\text{-dioxido-1,5-dicarboxylate}$), and $\text{Mg}_2(\text{dobpdc})$ ($\text{dobpdc}^{4-} = 4,4'\text{-dioxido-3,3'-biphenyl-4,4'-dicarboxylate}$). The cross-pore diameters in these MOFs are 15.4 Å, 14.9 Å, and 22.8 Å, respectively. Gray, white, red, and green spheres represent carbon, hydrogen, oxygen, and magnesium, respectively.

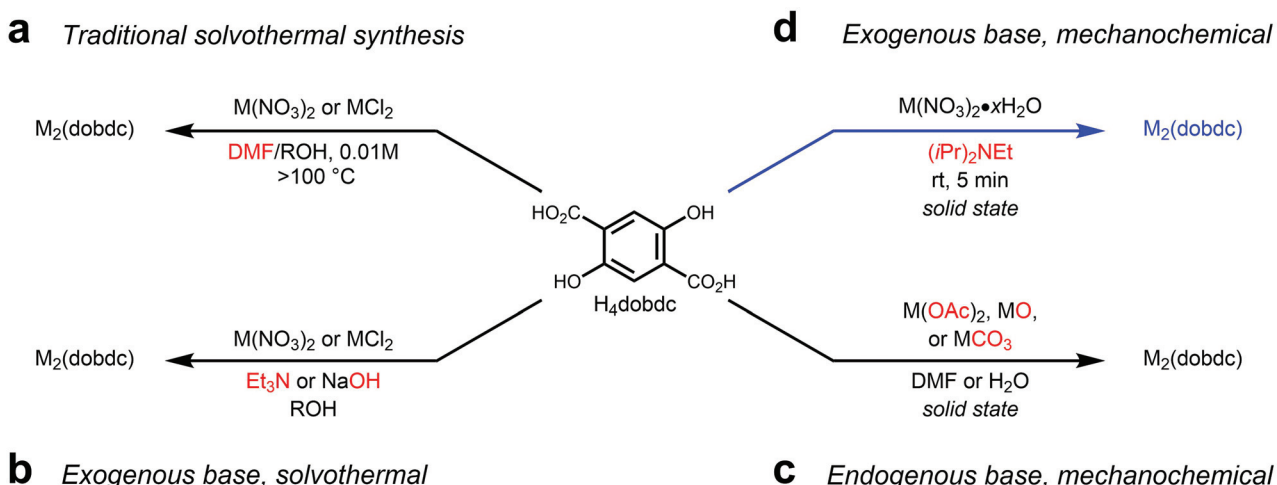


Fig. 2 Overview of methods for the synthesis of MOF-74 analogues, with the source of base highlighted in red. (a) Traditional solvothermal synthesis using *N,N*-dimethylformamide (DMF); (b) solvothermal synthesis using exogenous organic or inorganic base; (c) mechanochemical synthesis using basic metal precursors, and (d) mechanochemical synthesis using exogenous organic base (this work, highlighted in blue).

a significant effect on framework crystallinity and polymorph formation, as has been observed previously for MOF-74 analogues.^{30–34} Recently, it has been shown that the base can be decoupled from the reaction solvent by instead employing metal salts bearing basic counteranions (*e.g.* acetate) under solvothermal conditions (not shown).^{35–40} More generally, it is possible to completely separate the base from the MOF precursors or solvent by utilizing exogenous organic⁴¹ or inorganic^{42,43} bases to prepare MOF-74 frameworks (Fig. 2b). Although these methods allow more synthetic control over framework formation, they still lead to significant solvent

waste. Therefore, while it is possible to avoid the use of amide solvents during the preparation of select MOF-74 analogues, the generation of significant waste limits the sustainability of these methods. In addition, isomeric and expanded MOF-74 analogues are still widely prepared using DMF-based solvothermal approaches (Fig. 1).

Recently, mechanochemical syntheses of MOFs in the solid state have emerged as promising alternatives to solvothermal methods because they avoid the generation of significant solvent waste.^{44–47} In particular, liquid assisted grinding (LAG), in which precursors solids are mechanically ground

together in the presence of a small amount of solvent, has been shown to enable MOF synthesis on large scale.^{47,48} Select MOF-74 frameworks can be prepared by LAG using basic metal precursors, albeit with variable crystallinities and surface areas (Fig. 2c).^{49,50} Building upon this precedent, we hypothesized that we could mechanochemically synthesize MOF-74 frameworks using a liquid exogenous base, such as Hünig's base (*N*, *N*-diisopropylethylamine), to completely decouple the base from the metal precursor (Fig. 2d).^{49,50} In these reactions, Hünig's base would play a dual role as both the base to enable MOF formation as well as the liquid to assist in mechanical grinding. Herein, we demonstrate that LAG with Hünig's base does in fact allow for the preparation of high-quality MOF-74 frameworks in a scalable and sustainable manner. In addition, we show that this strategy can be readily translated to prepare isomeric and expanded MOF-74 analogues in the solid state for the first time.

Results and discussion

We began exploring the mechanochemical synthesis of MOF-74 analogues with exogenous base by simply grinding an excess of $Mg(NO_3)_2 \cdot 6H_2O$, the most commonly used metal precursor to prepare Mg-based MOF-74 analogues,^{7,13,14,19} and H_4dobdc together for 5 min at room temperature using a mortar and pestle (see ESI or ESI section 2† for details). Unsurprisingly due to the lack of a sufficiently strong base, $Mg_2(dobdc)$ did not form under these conditions. However, the addition of 4.4 equiv. of Hünig's base to the solid mixture led to the clean formation of nanocrystalline $Mg_2(dobdc)$, as confirmed by powder X-ray diffraction (Fig. 3, red curve; see ESI section 3† for details). Hünig's base was chosen because it possesses similar basicity ($pK_b = 3.2$) to dimethylamine ($pK_b = 3.3$) and triethylamine ($pK_b = 3.2$), which have previously been used to prepare MOF-74 analogues,^{6,41} but is significantly less coordinating and volatile. This result confirms that the combination of organic linker, metal salt, and amine base is sufficient to prepare $Mg_2(dobdc)$ in the solid state.

In order to standardize our mechanochemical synthesis, we employed a ball mill to prepare $Mg_2(dobdc)$ with more consistent grinding (see ESI section 2† for details).⁵¹ Using tungsten carbide vessels and balls ($\phi = 2.0$ mm) and a milling rate of 600 rpm, we successfully prepared $Mg_2(dobdc)$ on 2 mmol scale (~ 0.5 g) at room temperature in only 5 min, as confirmed by powder X-ray diffraction and IR spectroscopy (Fig. 3, blue curve). Notably, the crystallinity of $Mg_2(dobdc)$ synthesized using a ball mill was superior to that prepared using a mortar and pestle. We were able to further scale up this simple method to prepare $Mg_2(dobdc)$ on 8 mmol (~ 2.0 g) scale with similar results (Fig. 3, green curve). It should be noted that grinding times longer than 5 min led to a significant reduction in crystallinity, indicating that reaction time likely has a significant impact on the observed crystallite size. As a result, a standard reaction time of 5 min was used for subsequent experiments.

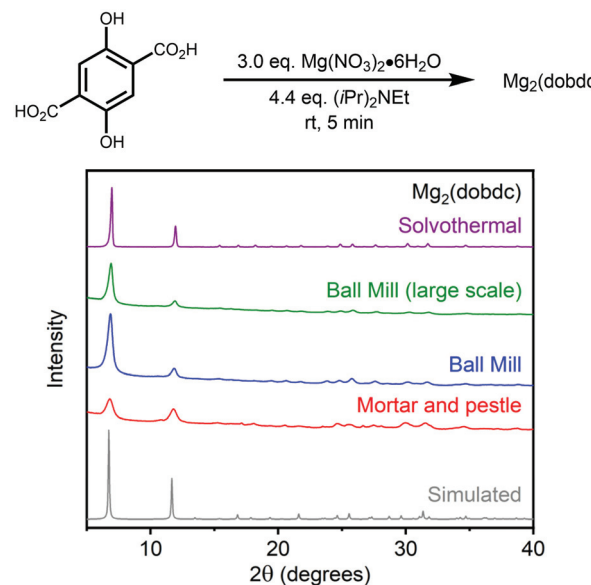


Fig. 3 Powder X-ray diffraction (PXRD) patterns ($\lambda = 1.5406 \text{ \AA}$) of $Mg_2(dobdc)$ prepared under mechanochemical conditions with a mortar and pestle (red) or ball mill (blue, green) and $Mg_2(dobdc)$ prepared under standard solvothermal conditions (purple).⁵² The simulated pattern based on the previously reported single-crystal X-ray diffraction structure of the isostructural framework $Zn_2(dobdc)$ is included for reference (gray).⁵³

To evaluate whether mechanochemical synthesis produces MOF of comparable porosity to material prepared under solvothermal conditions,^{12,52} we soaked the large-scale samples of $Mg_2(dobdc)$ in methanol at 65 °C, changing the solvent every day for three days. Digestion of the samples using DCl (35 wt% in D_2O) in $DMSO-d_6$ and analysis by 1H NMR confirmed that soaking in methanol is sufficient to remove residual Hünig's base and ammonium salts from the framework pores (ESI Fig. S27†). Next, these samples were desolvated at 180 °C under high vacuum to remove residual methanol. Importantly, the measured N_2 adsorption isotherms of these materials at 77 K are comparable to reference material prepared under solvothermal conditions (Fig. 4).⁵² In particular, the Langmuir surface areas of $Mg_2(dobdc)$ prepared on 2 mmol scale ($1852 \pm 53 \text{ m}^2 \text{ g}^{-1}$, blue circles) and 8 mmol scale ($1992 \pm 49 \text{ m}^2 \text{ g}^{-1}$, green triangles) using a ball mill are similar to MOF prepared under solvothermal conditions ($1914 \text{ m}^2 \text{ g}^{-1}$, purple squares).⁵² These results are summarized in Table 1 and confirm that high-quality $Mg_2(dobdc)$ can be prepared by mechanochemical synthesis using exogenous organic base.

We next evaluated the generality of this mechanochemical strategy towards the synthesis of other $M_2(dobdc)$ congeners (see ESI sections 4–8 and 12† for details). Gratifyingly, the corresponding $M_2(dobdc)$ ($M = Mn, Co, Ni, Cu, Zn$) frameworks could be prepared on ~ 0.5 g scale following the same procedure outlined above, as confirmed by powder X-ray diffraction (Fig. 5) and Infrared spectroscopy (ESI sections 4–8†). Qualitative analysis of these powder X-ray diffraction patterns using the Scherrer equation ($K = 0.89$, $\lambda = 1.5406 \text{ \AA}$) suggests

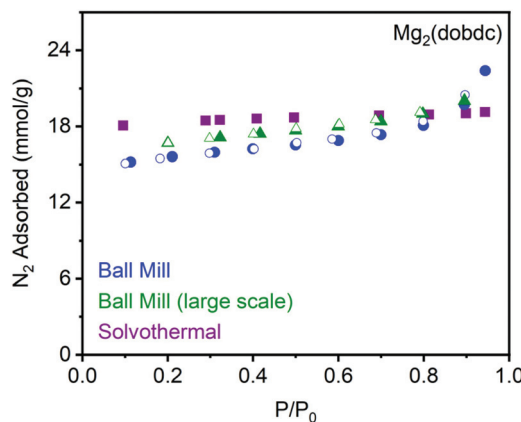


Fig. 4 Comparison of the 77 K N₂ adsorption (filled) and desorption (open) isotherms of Mg₂(dobdc) prepared under mechanochemical conditions (blue circles, green triangles) and standard solvothermal conditions (purple squares).⁵

Table 1 Summary of average crystalline domain sizes and Langmuir surface areas for MOF-74 analogues

Framework	Average crystalline domain size ^a (nm)	Langmuir surface area ^b (m ² g ⁻¹)	Solvothermal langmuir surface area ^b (m ² g ⁻¹)
Mg ₂ (dobdc)	21 (51) ^c	1992 ± 49	1914
Mn ₂ (dobdc)	28	385 ± 14 ^d	1797 ¹²
Co ₂ (dobdc)	23	1334 ± 51	1438 ¹²
Ni ₂ (dobdc)	13	1281 ± 48	1574 ¹²
Cu ₂ (dobdc)	39	1115 ± 6	1515 ¹²
Zn ₂ (dobdc)	21 (15) ^e	1204 ± 16	1277 ¹²
Mg ₂ (<i>m</i> -dobdc)	22	1793 ± 50	Nonporous ⁵⁴
Mg ₂ (dobpdc)	10	3137 ± 71	3780 ¹⁴

^a Determined by the Scherrer equation using the first PXRD reflection.

^b Determined from N₂ adsorption isotherm at 77 K. ^c From solvothermal synthesis.⁵² ^d Framework oxidized in air. ^e Prepared using 2,6-lutidine as base in place of Hünig's base.

that the average crystalline domain size of all prepared MOFs are in the nanocrystalline regime^{38,41} and smaller than MOF prepared under solvothermal conditions (Table 1).⁵² Soaking the as-synthesized M₂(dobdc) frameworks in methanol followed by desolvation under vacuum at 180 °C allowed us to evaluate their 77 K N₂ surface areas (Table 1; see ESI sections 4–8† for details). Similar to the Mg congener, Co₂(dobdc) and Zn₂(dobdc) produced under mechanochemical conditions possess Langmuir surface areas close to those reported for frameworks prepared under solvothermal conditions (Table 1).¹² Although the Langmuir surface area of Ni₂(dobdc) is slightly lower than expected, nanocrystalline samples of MOF-74 variants have previously been shown to have low surface areas due to a higher prevalence of defects.³⁸ Similarly, the unexpectedly low Langmuir surface area of Cu₂(dobdc) may arise due to the presence of defects or amorphous contaminants, in line with the known difficulty of preparing high

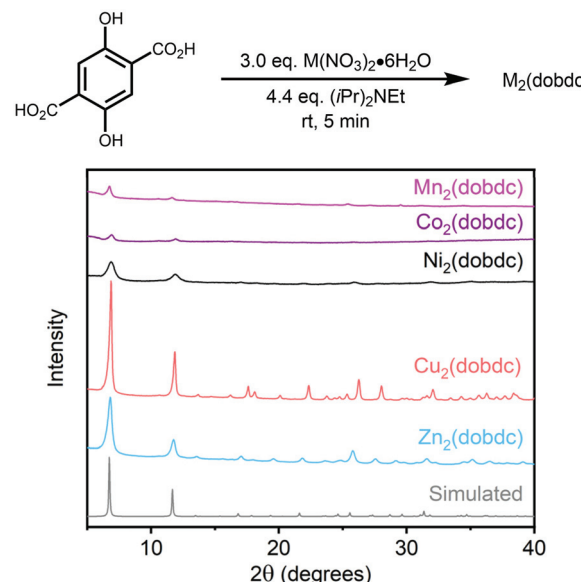


Fig. 5 Powder X-ray diffraction patterns ($\lambda = 1.5406 \text{ \AA}$) of M₂(dobdc) (M = Mn, Co, Ni, Cu, Zn) prepared under mechanochemical conditions. The simulated pattern based on the previously reported single-crystal X-ray diffraction structure of the framework Zn₂(dobdc) is included for reference.⁵³

surface area samples of this framework.¹² Unfortunately, the porosity of Mn₂(dobdc) prepared herein was quite low, likely due to its oxidative degradation in air upon filtration. Nonetheless, these results confirm that of M₂(dobdc) variants generally can be prepared using this mechanochemical strategy.

While the mechanochemical synthesis of selected M₂(dobdc) variants has been previously described using basic metal salts,^{49,50} the solid-state synthesis of related M₂(*m*-dobdc) (*m*-dobdc⁴⁺ = 2,4-dioxidobenzene-1,5-dicarboxylate) and M₂(dobpdc) (dobpdc⁴⁺ = 4,4'-dioxidobiphenyl-3,3'-dicarboxylate) frameworks (Fig. 1) has not, to the best of our knowledge, been reported to date. The sustainable synthesis of these frameworks is desirable because they are promising for H₂ storage²² and CO₂ capture,²¹ respectively. Therefore, we further extended our methodology by preparing Mg₂(*m*-dobdc) and Mg₂(dobpdc) in a ball mill using Hünig's base (see ESI sections 9 and 10† for details). In both cases, the successful formation of these frameworks was confirmed by powder X-ray diffraction (Fig. 6) and Infrared spectroscopy (ESI sections 9 and 10†). Our preliminary results suggest that Co₂(dobpdc) and Zn₂(dobpdc) can also be prepared under these conditions (ESI Fig. S28 and 29†). Using the Scherrer equation, we confirmed that the average crystalline domain size of Mg₂(*m*-dobdc) is similar to that of Mg₂(dobdc), which is understandable given their structural similarity (Table 1). In contrast, smaller crystallites of Mg₂(dobpdc) were obtained. Consistent with our findings for Ni₂(dobdc), the 77 K N₂ Langmuir surface area of Mg₂(dobpdc) prepared herein is lower than that for material prepared under solvothermal conditions (Table 1).

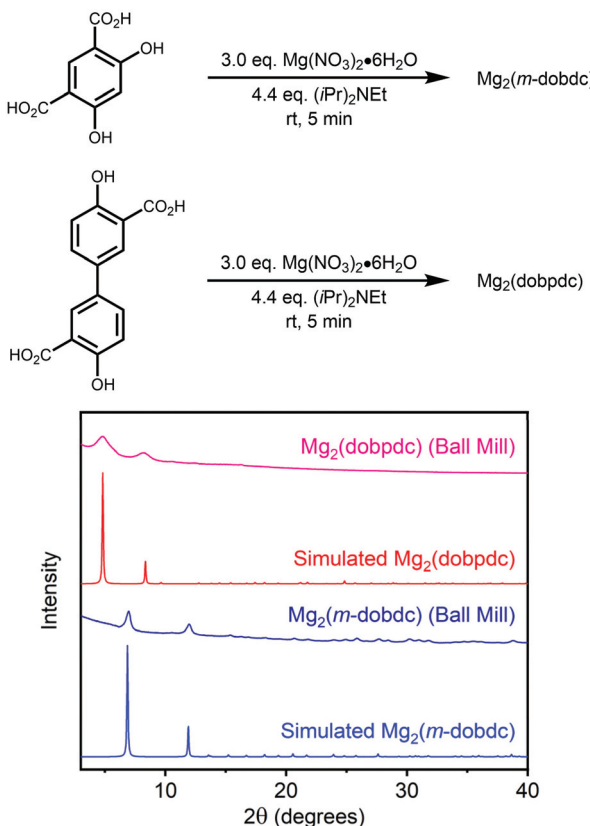


Fig. 6 Powder X-ray diffraction patterns ($\lambda = 1.5406 \text{ \AA}$) of $\text{Mg}_2(m\text{-dobdc})$ (blue) and $\text{Mg}_2(\text{dobpdc})$ (red) prepared under mechanochemical conditions. The simulated patterns based on the previously reported single-crystal X-ray diffraction structures of the isostructural frameworks $\text{Co}_2(m\text{-dobdc})^{54}$ and $\text{Zn}_2(\text{dobpdc})^{56}$ are included for reference.

and ESI Fig. S26†).¹⁴ Importantly, the $\text{Mg}_2(m\text{-dobdc})$ synthesized herein was found to be highly porous ($1793 \pm 50 \text{ m}^2 \text{ g}^{-1}$), with a surface area similar to that of the isomeric framework $\text{Mg}_2(\text{dobdc})$ (Table 1 and ESI Fig. S23†). This is in contrast the material prepared under solvothermal conditions, which was previously reported to be non-porous due to the difficulty of removing residual DMF from the pores.^{21,54} To the best of our knowledge, this is the first report of the permanent porosity of $\text{Mg}_2(m\text{-dobdc})$, further expanding the limited pool of Mg-based frameworks with coordinatively unsaturated metal centers.⁵⁵ Overall, LAG with Hünig's base appears to be a general protocol for the synthesis of MOF-74 analogues.

To gain preliminary mechanistic insight into the role of organic base in MOF formation, we explored mechanochemical synthesis using different nitrogen bases (Fig. 7; see ESI section 8† for details). For these studies, $\text{Zn}_2(\text{dobdc})$ was chosen because its mechanism of formation under mechanochemical conditions has previously been shown to proceed by step-wise deprotonation of the carboxylates of the linker followed by the less acidic phenols.⁵⁰ As with $\text{Mg}_2(\text{dobdc})$, no MOF formation was observed in the absence of base. Interestingly, when the weak organic base pyridine ($\text{p}K_b = 8.8$) was employed for LAG, $\text{Zn}_2(\text{dobdc})$ was not observed. This is

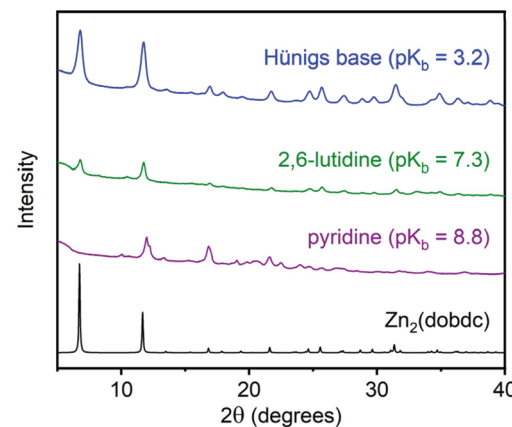


Fig. 7 Powder X-ray diffraction patterns ($\lambda = 1.5406 \text{ \AA}$) of $\text{Zn}_2(\text{dobdc})$ prepared under mechanochemical conditions with different organic bases. The simulated pattern based on the previously reported single-crystal X-ray diffraction structure of $\text{Zn}_2(\text{dobdc})$ is included for reference.⁵³

likely because pyridine is insufficiently basic to deprotonate the phenols of the organic linker, although we cannot rule out that the coordinating nature of pyridine also plays a role in inhibiting MOF formation. Consistently, when the stronger and more sterically-hindered organic base 2,6-lutidine ($\text{p}K_b = 7.3$) was used instead, we were able to successfully prepare $\text{Zn}_2(\text{dobdc})$. However, the use of even more basic Hünig's base ($\text{p}K_b = 3.2$) led to more crystalline material. This is likely because Hünig's base is sufficiently basic to deprotonate both the carboxylic acid ($\text{p}K_{\text{a}1} \approx 3.0$) and phenol ($\text{p}K_{\text{a}2} \approx 13.8$) of the linker to some degree. These results confirm that base of sufficient strength to deprotonate both the phenol and carboxylic acid of the linker are required to form MOF, suggesting that the strength of the base is a potential handle for controlling MOF formation. Further studies are underway in our laboratory to explore the role of organic base in MOF formation.

Conclusions

We report here the development of a new mechanochemical synthesis of MOF-74 variants using Hünig's base as both the liquid for LAG and the base required to facilitate MOF formation. This mechanochemical method is general, enables access to a range of crystalline frameworks, and increases the available methods for the sustainable synthesis of MOFs.⁵⁷ Importantly, this mechanochemical method was employed to bypass the use of DMF and prepare highly porous $\text{Mg}_2(m\text{-dobdc})$ for the first time. Therefore, this new strategy should prove beneficial for the scalable synthesis of both known and new porous MOF-74 variants. Current efforts in our laboratory are focused on exploring the mechanism of this novel LAG strategy and extending it to the synthesis of other industrially relevant MOFs.

Conflicts of interest

The authors have no conflicts of interest to declare.

Acknowledgements

The authors acknowledge Cornell University for financial support of this work. Z. W. thanks Nankai University and Z. L. thanks Beihang University for additional financial support. The authors thank Prof. Francis DiSalvo (Cornell University) for the use of the ball mill in his laboratory. The powder X-ray diffraction pattern of $\text{Co}_2(\text{dobpdc})$ was collected using the mail-in service at beamline 11-BM of the Advanced Photon Source. Use of the Advanced Photon Source at Argonne National Laboratory was supported by the U. S. Department of Energy, Office of Science, Office of Basic Energy Sciences, under Contract No. DE-AC02-06CH11357. ^1H NMR data were collected on a Bruker INOVA 500 MHz spectrometer that was purchased with support from the National Science Foundation (CHE-1531632). We thank Dr Arjun Halder (Cornell University) for assistance with the preparation of this manuscript.

Notes and references

- 1 H. Furukawa, K. E. Cordova, M. O'Keeffe and O. M. Yaghi, *Science*, 2013, **341**, 1230444–1230444.
- 2 C. H. Hendon, A. J. Rieth, M. D. Korzyński and M. Dincă, *ACS Cent. Sci.*, 2017, **3**, 554–563.
- 3 J. N. Hall and P. Bollini, *React. Chem. Eng.*, 2019, **4**, 207–222.
- 4 A. Yadav and P. Kanoo, *Chem. – Asian J.*, 2019, **14**, 3531–3551.
- 5 Z. Hu and D. Zhao, *CrystEngComm*, 2017, **19**, 4066–4081.
- 6 N. L. Rosi, J. Kim, M. Eddaoudi, B. Chen, M. O'Keeffe and O. M. Yaghi, *J. Am. Chem. Soc.*, 2005, **127**, 1504–1518.
- 7 S. R. Caskey, A. G. Wong-Foy and A. J. Matzger, *J. Am. Chem. Soc.*, 2008, **130**, 10870–10871.
- 8 W. Zhou, H. Wu and T. Yildirim, *J. Am. Chem. Soc.*, 2008, **130**, 15268–15269.
- 9 P. D. C. Dietzel, Y. Morita, R. Blom and H. Fjellvåg, *Angew. Chem., Int. Ed.*, 2005, **44**, 6354–6358.
- 10 P. D. C. Dietzel, B. Panella, M. Hirscher, R. Blom and H. Fjellvåg, *Chem. Commun.*, 2006, 959.
- 11 R. Sanz, F. Martínez, G. Orcajo, L. Wojtas and D. Briones, *Dalton Trans.*, 2013, **42**, 2392–2398.
- 12 W. L. Queen, M. R. Hudson, E. D. Bloch, J. A. Mason, M. I. Gonzalez, J. S. Lee, D. Gygi, J. D. Howe, K. Lee and T. A. Darwish, *Chem. Sci.*, 2014, **5**, 4569–4581.
- 13 M. T. Kapelewski, S. J. Geier, M. R. Hudson, D. Stück, J. A. Mason, J. N. Nelson, D. J. Xiao, Z. Hulvey, E. Gilmour, S. A. FitzGerald, M. Head-Gordon, C. M. Brown and J. R. Long, *J. Am. Chem. Soc.*, 2014, **136**, 12119–12129.
- 14 P. J. Milner, J. D. Martell, R. L. Siegelman, D. Gygi, S. C. Weston and J. R. Long, *Chem. Sci.*, 2018, **9**, 160–174.
- 15 S. Peng, B. Bie, Y. Sun, M. Liu, H. Cong, W. Zhou, Y. Xia, H. Tang, H. Deng and X. Zhou, *Nat. Commun.*, 2018, **9**, 1293.
- 16 J. Zheng, R. S. Vemuri, L. Estevez, P. K. Koech, T. Varga, D. M. Camaioni, T. A. Blake, B. P. McGrail and R. K. Motkuri, *J. Am. Chem. Soc.*, 2017, **139**, 10601–10604.
- 17 D. J. Xiao, J. Oktawiec, P. J. Milner and J. R. Long, *J. Am. Chem. Soc.*, 2016, **138**, 14371–14379.
- 18 D. J. Levine, T. Runčevski, M. T. Kapelewski, B. K. Keitz, J. Oktawiec, D. A. Reed, J. A. Mason, H. Z. H. Jiang, K. A. Colwell, C. M. Legendre, S. A. FitzGerald and J. R. Long, *J. Am. Chem. Soc.*, 2016, **138**, 10143–10150.
- 19 T. M. McDonald, J. A. Mason, X. Kong, E. D. Bloch, D. Gygi, A. Dani, V. Crocellà, F. Giordanino, S. O. Odoh, W. S. Drisdell, B. Vlaisavljevich, A. L. Dzubak, R. Poloni, S. K. Schnell, N. Planas, K. Lee, T. Pascal, L. F. Wan, D. Prendergast, J. B. Neaton, B. Smit, J. B. Kortright, L. Gagliardi, S. Bordiga, J. A. Reimer and J. R. Long, *Nature*, 2015, **519**, 303–308.
- 20 H. Deng, S. Grunder, K. E. Cordova, C. Valente, H. Furukawa, M. Hmadeh, F. Gandara, A. C. Whalley, Z. Liu, S. Asahina, H. Kazumori, M. O'Keeffe, O. Terasaki, J. F. Stoddart and O. M. Yaghi, *Science*, 2012, **336**, 1018–1023.
- 21 T. M. McDonald, W. R. Lee, J. A. Mason, B. M. Wiers, C. S. Hong and J. R. Long, *J. Am. Chem. Soc.*, 2012, **134**, 7056–7065.
- 22 M. T. Kapelewski, T. Runčevski, J. D. Tarver, H. Z. H. Jiang, K. E. Hurst, P. A. Parilla, A. Ayala, T. Gennett, S. A. FitzGerald, C. M. Brown and J. R. Long, *Chem. Mater.*, 2018, **30**, 8179–8189.
- 23 G. Calleja, R. Sanz, G. Orcajo, D. Briones, P. Leo and F. Martínez, *Catal. Today*, 2014, **227**, 130–137.
- 24 H.-F. Yao, Y. Yang, H. Liu, F.-G. Xi and E.-Q. Gao, *J. Mol. Catal. A: Chem.*, 2014, **394**, 57–65.
- 25 D. J. Xiao, E. D. Bloch, J. A. Mason, W. L. Queen, M. R. Hudson, N. Planas, J. Borycz, A. L. Dzubak, P. Verma, K. Lee, F. Bonino, V. Crocellà, J. Yano, S. Bordiga, D. G. Truhlar, L. Gagliardi, C. M. Brown and J. R. Long, *Nat. Chem.*, 2014, **6**, 590–595.
- 26 D. DeSantis, J. A. Mason, B. D. James, C. Houchins, J. R. Long and M. Veenstra, *Energy Fuels*, 2017, **31**, 2024–2032.
- 27 P. A. Julien, C. Mottillo and T. Friščić, *Green Chem.*, 2017, **19**, 2729–2747.
- 28 Y. Sun and H.-C. Zhou, *Sci. Technol. Adv. Mater.*, 2015, **16**, 054202.
- 29 Y.-R. Lee, J. Kim and W.-S. Ahn, *Korean J. Chem. Eng.*, 2013, **30**, 1667–1680.
- 30 D. Kim and A. Coskun, *Angew. Chem., Int. Ed.*, 2017, **56**, 5071–5076.
- 31 F. Luo, C. Yan, L. Dang, R. Krishna, W. Zhou, H. Wu, X. Dong, Y. Han, T.-L. Hu, M. O'Keeffe, L. Wang, M. Luo, R.-B. Lin and B. Chen, *J. Am. Chem. Soc.*, 2016, **138**, 5678–5684.

32 S. E. Henkelis, L. J. McCormick, D. B. Cordes, A. M. Z. Slawin and R. E. Morris, *Inorg. Chem. Commun.*, 2016, **65**, 21–23.

33 A. Douvali, G. S. Papaefstathiou, M. P. Gullo, A. Barbieri, A. C. Tsipis, C. D. Malliakas, M. G. Kanatzidis, I. Papadas, G. S. Armatas, A. G. Hatzidimitriou, T. Lazarides and M. J. Manos, *Inorg. Chem.*, 2015, **54**, 5813–5826.

34 P. D. C. Dietzel, R. Blom and H. Fjellvåg, *Eur. J. Inorg. Chem.*, 2008, **2008**, 3624–3632.

35 R. L. Siegelman, P. J. Milner, A. C. Forse, J.-H. Lee, K. A. Colwell, J. B. Neaton, J. A. Reimer, S. C. Weston and J. R. Long, *J. Am. Chem. Soc.*, 2019, **141**, 13171–13186.

36 L. Maserati, S. M. Meckler, J. E. Bachman, J. R. Long and B. A. Helms, *Nano Lett.*, 2017, **17**, 6828–6832.

37 L. Garzón-Tovar, A. Carné-Sánchez, C. Carbonell, I. Imaz and D. Maspoch, *J. Mater. Chem. A*, 2015, **3**, 20819–20826.

38 M. Díaz-García, Á. Mayoral, I. Díaz and M. Sánchez-Sánchez, *Cryst. Growth Des.*, 2014, **14**, 2479–2487.

39 S. Cadot, L. Veyre, D. Luneau, D. Farrusseng and E. Alessandra Quadrelli, *J. Mater. Chem. A*, 2014, **2**, 17757–17763.

40 D. J. Tranchemontagne, J. R. Hunt and O. M. Yaghi, *Tetrahedron*, 2008, **64**, 8553–8557.

41 J. E. Bachman, Z. P. Smith, T. Li, T. Xu and J. R. Long, *Nat. Mater.*, 2016, **15**, 845–849.

42 S. M. Vornholt, S. E. Henkelis and R. E. Morris, *Dalton Trans.*, 2017, **46**, 8298–8303.

43 M. Sánchez-Sánchez, N. Getachew, K. Díaz, M. Díaz-García, Y. Chebude and I. Díaz, *Green Chem.*, 2015, **17**, 1500–1509.

44 D. Chen, J. Zhao, P. Zhang and S. Dai, *Polyhedron*, 2019, **162**, 59–64.

45 S. L. James, C. J. Adams, C. Bolm, D. Braga, P. Collier, T. Friščić, F. Grepioni, K. D. M. Harris, G. Hyett, W. Jones, A. Krebs, J. Mack, L. Maini, A. G. Orpen, I. P. Parkin, W. C. Shearouse, J. W. Steed and D. C. Waddell, *Chem. Soc. Rev.*, 2012, **41**, 413–447.

46 M. Klimakow, P. Klobes, A. F. Thünemann, K. Rademann and F. Emmerling, *Chem. Mater.*, 2010, **22**, 5216–5221.

47 T. Friščić, *J. Mater. Chem.*, 2010, **20**, 7599.

48 P. J. Beldon, L. Fábián, R. S. Stein, A. Thirumurugan, A. K. Cheetham and T. Friščić, *Angew. Chem., Int. Ed.*, 2010, **49**, 9640–9643.

49 G. Ayoub, B. Karadeniz, A. J. Howarth, O. K. Farha, I. Đilović, L. S. Germann, R. E. Dinnebier, K. Užarević and T. Friščić, *Chem. Mater.*, 2019, **31**, 5494–5501.

50 P. A. Julien, K. Užarević, A. D. Katsenis, S. A. J. Kimber, T. Wang, O. K. Farha, Y. Zhang, J. Casaban, L. S. Germann, M. Etter, R. E. Dinnebier, S. L. James, I. Halasz and T. Friščić, *J. Am. Chem. Soc.*, 2016, **138**, 2929–2932.

51 J. L. Howard, Q. Cao and D. L. Browne, *Chem. Sci.*, 2018, **9**, 3080–3094.

52 M. L. Aubrey, R. Ameloot, B. M. Wiers and J. R. Long, *Energy Environ. Sci.*, 2014, **7**, 667.

53 P. D. C. Dietzel, R. E. Johnsen, R. Blom and H. Fjellvåg, *Chem. – Eur. J.*, 2008, **14**, 2389–2397.

54 J. E. Bachman, M. T. Kapelewski, D. A. Reed, M. I. Gonzalez and J. R. Long, *J. Am. Chem. Soc.*, 2017, **139**, 15363–15370.

55 D. Banerjee, H. Wang, B. J. Deibert and J. Li, in *The Chemistry of Metal-Organic Frameworks: Synthesis, Characterization, and Applications*, ed. S. Kaskel, Wiley-VCH Verlag GmbH & Co. KGaA, Weinheim, Germany, 2016, pp. 73–103.

56 R. L. Siegelman, T. M. McDonald, M. I. Gonzalez, J. D. Martell, P. J. Milner, J. A. Mason, A. H. Berger, A. S. Bhowm and J. R. Long, *J. Am. Chem. Soc.*, 2017, **139**, 10526–10538.

57 P. Li, F.-F. Cheng, W.-W. Xiong and Q. Zhang, *Inorg. Chem. Front.*, 2018, **11**, 2693–2708.